Journal of Hazardous Materials 172 (2009) 1193–1197

Contents lists available at ScienceDirect

Journal of Hazardous Materials

journal homepage: www.elsevier.com/locate/jhazmat

Bi_2WO_6@carbon/Fe_3O_4 microspheres: Preparation, growth mechanism and application in water treatment

Ling Zhang, Wenzhong Wang*, Meng Shang, Songmei Sun, Jiehui Xu

State Key Laboratory of High Performance Ceramics and Superfine Microstructure, Shanghai Institute of Ceramics, Chinese Academy of Sciences, 1295 Dingxi Road, Shanghai 200050, PR China

ARTICLE INFO

Article history:
Received 23 June 2009
Received in revised form 27 July 2009
Accepted 28 July 2009
Available online 4 August 2009

Keywords:
Carbon
Coating
Bi_2WO_6
Fe_3O_4
Photocatalysis

ABSTRACT

A novel Bi_2WO_6@carbon/Fe_3O_4 nanostructure with a thin carbon interlayer was reported. Reactive carbon interlayer was introduced as a key component for the growth of Bi_2WO_6 nanoplates on the magnetic Fe_3O_4 microsphere. After the carbon layer was oxidized by the $KMnO_4$ in the basic solution, Bi^{3+} ions could be adsorbed by the as produced $-COO^-$ groups and thus Bi_2WO_6 nanoplates grew on the surface of the carbon/Fe_3O_4 microspheres preferentially. The as-prepared nanocomposite, which could be easily recovered by a magnet, exhibited high efficiency in the photocatalytic decomposition of phenol with the assistance of H_2O_2. The combination of photocatalyst and magnetic materials through a reactive carbon interlayer opens up a new route for the fabrication of complex and multifunctional nanostructure.

1. Introduction

Complex nanostructures have attracted much attention because of their multifunction or even new applications originated from multicomponents [1–6]. Among them, iron oxides based nanostructures have been extensively studied due to their special magnetic properties. They could be combined with other materials to obtain multifunctional nanocomposites [7–10]. The immobilization of transition metals or their oxides on the magnetic microspheres (MS) could allow them to retain high activity and enable facile separation from the reaction media. Complex nanostructures, such as iron oxide/SiO_2 [11], iron oxide/Au(Ag) [12–14], Fe_3O_4/quantum dot (CdSe, CdTe) [15–17], and Fe_3O_4/TiO_2 [18–21] have been successfully prepared by a variety of methods. However, the combination of different building blocks into an ordered nanostructure is considerably more difficult, especially for the components with different crystalline structures. To develop a reliable synthetic method for fabricating multifunctional nanocomposite with designed components and controlled morphologies is still a big challenge.

Recently, surface coating or surface modification has been recognized as one of the most intriguing methods to build complex nanostructures [22,23]. Coating or modification can alter the surface charge and reactivity of the substrate. Compared to the generally used SiO_2 material, carbon is a special and unique material for coating treatment and core/shell type nanostructures could be thus achieved. Activated –COOH groups could be easily introduced onto the carbon layer by oxidization treatment [24,25]. As a result, the carboxylic acid functional groups on the carbon layer could give rise to preferred sites of nucleation. Absorption of metal ions and following growth of the crystal on the surface of reactive carbon layer are easier than that the growth on the substrate directly. For example, Au, Ag, and Pt nanocrystals growing *in situ* on the carbon nanotubes have been realized after the carbon nanotubes oxidized by oxidants [26–28].

Herein, Bi_2WO_6 nanoplates have been chosen as a functional component for the preparation of magnetic nanocomposite for following two reasons. First, Bi_2WO_6 was found as an excellent photocatalyst which could transform solar energy into chemical energy [29,30]. Generally, photocatalytic reaction is processed in a suspension of the photocatalyst powders. Therefore it requires a largish further expense to separate the catalyst from large volumes of reaction solutions. Hence, producing a magnetic photocatalyst, combining magnetic iron oxide and photocatalyst Bi_2WO_6, is of emerging interest. Secondly, Bi_2WO_6 belongs to the Aurivillius family oxides with general formula $Bi_2A_{n-1}B_nO_{3n+3}$ (A: Ca, Sr, Ba, Pb, Bi, Na, K and B: Ti, Nb, Ta, Mo, W, Fe). With layer structure, they possess variously photochemical and electrical properties [31–34]. Conceiving the above reasons, if the layer structured Bi_2WO_6 nanoplates could couple with the cubic structured Fe_3O_4 nanoparticles, it is expected to constructing many core/shell type nanocomposites with novel

* Corresponding author. Tel.: +86 21 5241 5295; fax: +86 21 5241 3122.
E-mail address: wzwang@mail.sic.ac.cn (W. Wang).

0304-3894/$ – see front matter © 2009 Elsevier B.V. All rights reserved.
doi:10.1016/j.jhazmat.2009.07.123

optical, photocatalytic and electrical properties by the similar approach.

It is noted that Bi_2WO_6 hardly grow on the surface of iron oxide because of their tremendously different crystalline structures. By introducing a reactive carbon interlayer as the "bond", however, we developed a reliable and efficient synthetic approach to prepare the functional magnetic photocatalyst, Bi_2WO_6@carbon/Fe_3O_4 microspheres. After the oxidization treatment, carbon layer supplied active sites for the adsorption of Bi^{3+} ions, which is favorable for the growth of the Bi_2WO_6 nanoplates. The multifunctional microsphere was prepared via three steps: preparation of Fe_3O_4 microspheres; coating followed by chemical modification of the carbon layer on the magnetic Fe_3O_4 microspheres; and growth of Bi_2WO_6 nanoplates on the magnetic microspheres. Moreover, except the magnetism and photocatalysis, an advanced oxidation technologies (AOTs), Fenton process, was involved with this nanocomposite system. It could *in situ* generate highly potent chemical oxidants such as the hydroxyl radical, and represent an important class of environmental technologies [35,36]. Multipores in the as treated carbon layer of the composition are helpful for the Fe^{2+} ions from the Fe_3O_4 core to take part in the Fenton process, which could improve the efficiency of decomposition of the phenol solution.

2. Experimental

2.1. Preparation of Fe_3O_4 magnetic spheres (MS)

Fe_3O_4 spheres were synthesized by a modified solvothermal process in a polyol media according to the literature [37]. Typically, $FeCl_3{\cdot}6H_2O$ (1.35 g) and polyethylene glycol-20000 (1 g) were dissolved in 40 ml of ethylene glycol to form a clear solution. Sodium acetate (3.6 g) was added into the above solution under vigorous stirring. The as-prepared slurry was sealed into a Teflon-lined autoclave, and maintained at 200 °C for 8 h. After cooling to room temperature, the black precipitates (Fe_3O_4) were recovered magnetically.

2.2. Preparation of carbon/Fe_3O_4 magnetic spheres (CMS) and oxidative chemical treatment

Fe_3O_4 powders (0.2 g) and glucose (2.5 g) were dispersed in 40 mL H_2O. Then the solution was maintained at 180 °C for 10 h in a Teflon-sealed autoclave. The black products (CMS) were isolated by a magnet, washed by five cycles of magnetic separation/washing/redispersion, and dried at room temperature.

The as-prepared sample (0.2 g) was first kept in 30 ml of an alkalescent solution of potassium permanganate (1.0 g $KMnO_4$ and 0.5 g NaOH) for 30 min, and then heated to reflux under stirring for 1 h. Then the suspension was cooled to room temperature followed by an addition of l5 ml of 1 M HNO_3. The cleaning process was similar with the above-mentioned method. In the final step of rinsing, a drop of dilute HCl (2 M) solution was added to protonate the terminated groups of carbon surface. The products were collected and dried at room temperature.

2.3. Preparation of Bi_2WO_6@carbon/Fe_3O_4 magnetic spheres with a carbon interlayer (BCMS)

The mixture of 0.15 g of CMS powders (with or without chemical oxidation treatment) and 0.45 g of $Bi(NO_3)_3{\cdot}5H_2O$ was sonicated in 30 ml HNO_3 solution (0.4 M) for 15 min. The obtained suspension was aged for 2 h, followed by centrifugation and redispersion in 30 ml deionized water. Na_2WO_4 (0.33 g), sodium citrate (1 g), $Bi(NO_3)_3{\cdot}5H_2O$ (0.97 g) were added into 10 ml of HNO_3 and the mixture was vigorously stirred at room temperature for 10 min. The above two solutions were mixed together and the pH value of the solution was adjusted to 7.0. After this, the mixed solution was sealed into a Teflon-lined autoclave and maintained at 180 °C for 24 h. The grey-black products were isolated by a magnet, washed by five cycles of magnetic separation/washing/redispersion, and dried at room temperature. The products obtained by the CMS without the oxidative chemical treatment were labeled as BCMS1. Contrarily, the products obtained by the CMS with the oxidative chemical treatment were labeled as BCMS2.

2.4. Characterization

The phase compositions of the powder were identified using X-ray diffractometry (XRD, Model D/MAX-2550 V, Rigaku, Tokyo, Japan). The morphologies of the powder were examined using transmission electron microscopy (TEM, Model 2100, JEOL, Tokyo, Japan). Scanning electron microscopy images were collected on a JSM field-emission scanning electron microscope (SEM, model 6700F, Tokyo, Japan). Magnetic measurements carried out using a Physical Property Measurement System (PPMS) at room temperature. The as-prepared powders were taken into a capsule.

To test photocatalytic behavior of the as-synthesized samples, photodegradation of phenol in water is chosen as a probe reaction. Briefly, an amount of 0.2 g of the catalyst dispersed in 100 ml of the phenol aqueous solution (20 mg/l) were illuminated by a 500 W xenon lamp with a cut-off filter of ($\lambda \geq 420$ nm). The temperature of the system was controlled at room temperature by circulating cooling water. The prepared suspension was then magnetically stirred for about 30 min in the dark to achieve the adsorption/desorption equilibrium. In order to improve the reaction rate, small amount of H_2O_2 (0.1 ml, 30%) were added into the 100 ml phenol suspension (pH 3.0) under otherwise identical conditions. After reaction, the catalyst was separated by a magnet, and the reaction mixture was analyzed by UV–vis spectrometer (Hitachi U-3010) at wavelength of 270 nm.

3. Results and discussion

It was found that, without the carbon interlayer, the Bi_2WO_6 nanoplates could not directly grow on the surface of Fe_3O_4 microspheres due to the tremendously different crystalline structures. Bi_2WO_6 is one of the simplest Aurivillius oxides, possessing layered structure with the perovskite-like slab of WO_6, but the face centered cubic Fe_3O_4 belongs to the inverse spinel structure. The Bi_2WO_6 would grow into nanoplates naturally but not on the Fe_3O_4 substrate (data not shown). It is essential to induce a reactive interlayer to "bond" the two kinds of functional materials together. The synthesis of metal/carbon hybrid nanospheres by the hydrothermal reaction using glucose as carbon resource has been reported by Sun and Li [38]. The polysaccharides process of the glucose prefers to occur due to the catalytic role of the noble metal nanoparticles preexisted in the solution. It was also observed in the current study when the metal oxide, Fe_3O_4, was used as a catalytic center for the carbonization of the glucose. The crystalline nature, phase, and purity of the as-prepared CMS and BCMS were determined by X-ray diffraction (XRD). Fig. 1a shows the XRD pattern of the CMS sample. All the diffraction peaks could be indexed as face centered cubic (fcc) Fe_3O_4 (JCPDS card no. 65-3107). No other peak can be found in the composite, which indicates that the phase of Fe_3O_4 does not change even after the reaction at high-temperature. The broadened peak near 20° with a relatively low intensity could be attributed to amorphous carbon [39]. Further information about the structure of the carbon layer was obtained from FTIR investigation (detailed discussion in the following text). A representative XRD pattern of the as-prepared BCMS is shown in Fig. 1b. The results demonstrate

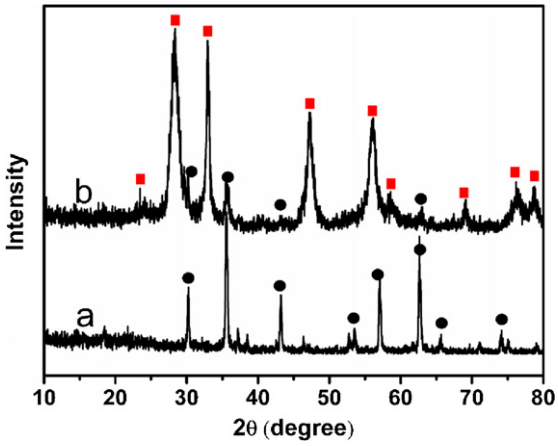

Fig. 1. Powder X-ray diffraction of the as-prepared nanocomposite: (a) carbon/Fe_3O_4 microsphere, (b) Bi_2WO_6@carbon/Fe_3O_4 microspheres. (●) The peaks from Fe_3O_4, (■) the peaks from Bi_2WO_6.

that the crystalline structure of Bi_2WO_6 nanoplates grown on the surface of CMS particles is identified as the russellite phase (JCPDS card no. 39-0256). No other phases from possible impurities were detected.

Fig. 2 shows the TEM and SEM images of the as-prepared products. As shown in Fig. 2a, the Fe_3O_4 microsphere with diameter of ~450 nm was encapsulated by a ~10 nm carbon layer. Fig. 2b and c shows the TEM images of the BCMS samples prepared under different pre-treatment conditions. When the carbon layer was not activated by the oxidative chemical treatment (Fig. 2b, recorded as BCMS1), there were few Bi_2WO_6 nanoplates growing on the CMS surface. It is a different case in Fig. 2c, however, the Bi_2WO_6 nanoplates covered the surfaces of the CMS closely (recorded as BCMS2) and some small plates even inserted into the surface. Close observation on the small plates inserting into the surface of the microsphere is shown in Fig. 2d. The thickness of the Bi_2WO_6 nanoplates was estimated to about several nanometers. More BCMS were shown in Fig. 2e. The mean size of the BCMS was in range of ~500–600 nm from the SEM measurement. It is larger than the size of CMS, which resulted from the Bi_2WO_6 nanoplates covered on the CMS.

The strategy used to obtain the BCMS is shown in Scheme 1, which can be divided into three steps: (1) the coating of the carbon layer on the MS through the polysaccharides process; (2) the introducing of –COOH groups on the carbon layer of the CMS by the oxidative chemical treatment; at the same time, some pores appeared in the thin carbon layer due to the oxidative eroding; (3) the transferring of Bi^{3+} ions from solution to the carbon layer by the adsorption between the Bi^{3+} and the $–COO^-$ groups and the successive growth of Bi_2WO_6 nanoplates. The amount of the Bi_2WO_6 nanoplates on the surface of CMS can be decided by the proceeding route. For the route A, there was a small quantity of –OH and –C=O groups on the surface of CMS, which are formed from non- or just partially dehydrated carbohydrates [38]. The concentration of Bi^{3+} ions near the surface of the CMS is higher than that in the solution due to the adsorption of the metal ion by these active groups. Bi_2WO_6 nanoplates tended to grow on the surface of carbon layer. However, for the route B, more –OH, –COOH groups were introduced onto the carbon layer of the CMS by the oxidative chemical treatment. The concentration of the Bi^{3+} ions near the carbon layer would be higher than that without the chemical treatment. It is worth to note that $KMnO_4$ in alkali was used as the oxidant instead of HNO_3 oxidants, since the former oxidizer is relatively mild and the Fe_3O_4 cores would not be eroded. Furthermore, the treated carbon layer had more defect sites which might act as

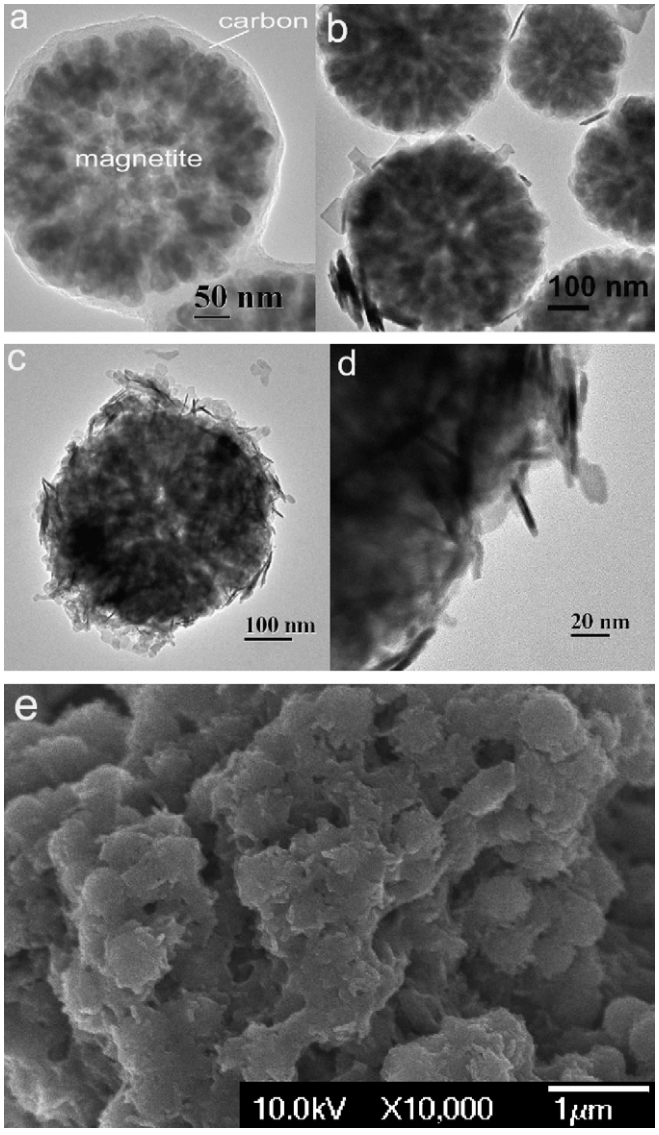

Fig. 2. TEM images: (a) as synthesized carbon/Fe_3O_4 microsphere with diameter of ~450 nm; (b) Bi_2WO_6@carbon/Fe_3O_4 microspheres (BCMS1) synthesized with the carbon layer; (c) Bi_2WO_6@carbon/Fe_3O_4 microspheres (BCMS2) synthesized with the activated carbon layer; (d) enlarged Bi_2WO_6 nanoplates inset on the nanosphere surface; (e) SEM images of BCMS2.

nucleation sites to induce heterogeneous nucleation on their surface owing to the lower critical nucleation concentration needed for heterogeneous nucleation than that nucleation on a relatively glazed carbon surface. All in all, the thin carbon interlayer, especially the treated carbon layer, supplied convenient sites for the nucleation and growth of Bi_2WO_6 nanoplates. The Bi^{2+} ions firstly were absorbed on the carbon layer and more Bi_2WO_6 nanoplates trended to grow on the surface of carbon layer rather than grow separately in the solution.

Fig. 3 showed the selected region of FTIR spectra of the CMS before (curve a) and after (curve b) the oxidative chemical treatment. The peaks of 1246, 1373 and 1458 cm^{-1} were assigned to the various vibration modes of –C–O–C– groups formed in the polysaccharides process [25,36]. The two peaks around 1728 and 1615 cm^{-1} were attributed to the stretching vibration mode of C=O, from –COOH group and aromatic ring structures, respectively [24]. After the chemical treatment, the relative strength of the peak around 1728 to the 1615 cm^{-1} increased largely (Fig. 3b). It implies that more –COOH groups were formed after the oxida-

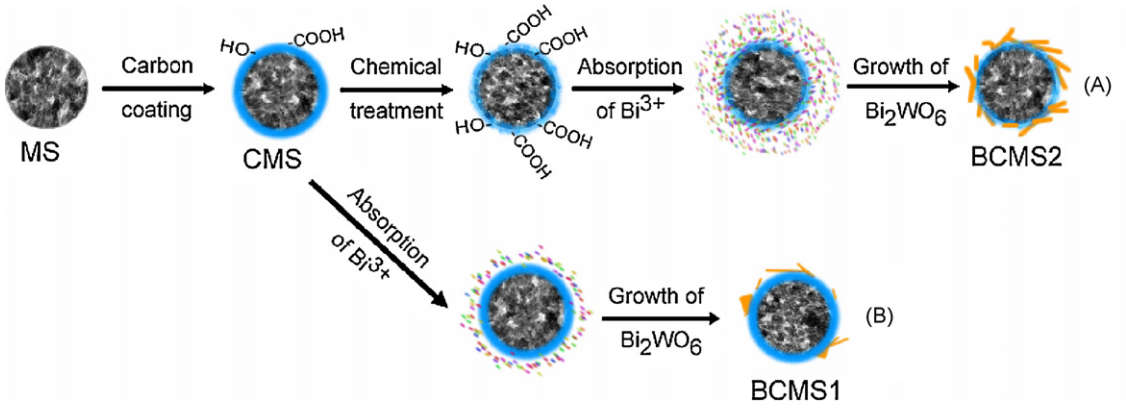

Scheme 1. Schematic illustration of the possible mechanism for synthesis of Bi_2WO_6@carbon/Fe_3O_4 microspheres products.

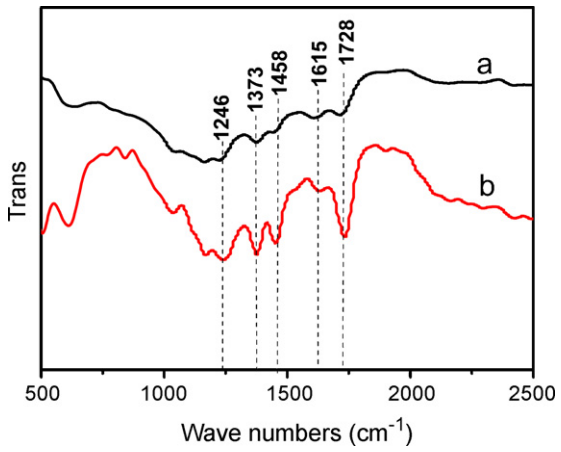

Fig. 3. Typical FTIR spectrum of as-prepared nanocomposite: (a) carbon/Fe_3O_4 microspheres without oxidative chemical treatment; (b) carbon/Fe_3O_4 microspheres treated with the $KMnO_4$ oxidation. The peaks of the major groups were indicated by lines (---).

tion step, which are usually helpful for the adsorption of the metal ions.

As shown in Fig. 4, the magnetic hysteresis loop indicated a typical ferromagnetic magnetization curve of BCMS. It can be seen that the magnetic saturation of BCMS nanocomposite is 37.4 emu/g, which is much lower than that of the corresponding pure Fe_3O_4 microspheres (81.9 emu/g) [37]. The magnetic separability of BCMS was tested in water by placing a magnet beside the glass beaker.

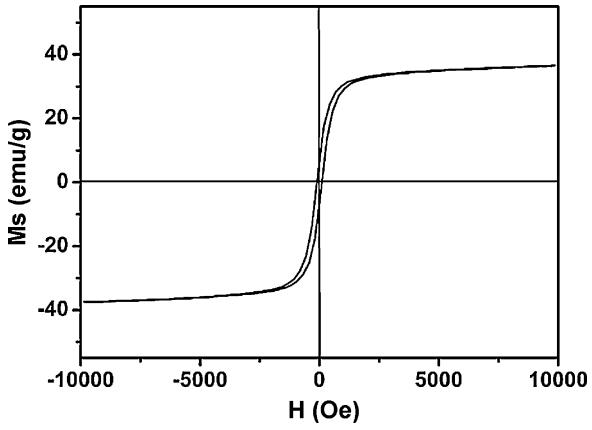

Fig. 4. Room-temperature magnetization curves of the obtained Bi_2WO_6@carbon/Fe_3O_4 microspheres.

The grey-black powders were attracted toward the magnet within 20 s, demonstrating directly that the as-prepared products possess magnetic properties. This will provide an easy and efficient way to separate magnetic photocatalyst from a suspension system under an external magnetic field.

Phenol is considered as one of the pollutants in water resources and its efficient removal from water is of great importance. The mechanism of the photocatalytic degradation of the pollutant by Bi_2WO_6 nanoplates has been well elucidated in the literature [39,40]. Herein, the as-prepared BCMS2 not only included the Bi_2WO_6 photocatalyst, but also supplied the Fe^{2+} ions to compose with the H_2O_2 as an advanced oxidation reagent, Fenton reagent. It is one of the most active systems for the water treatment. The Fe^{2+} ions, from the Fe_3O_4 core, could enter into the reaction solution through the pores in the amorphous and eroded carbon layer to assist the photocatalytic decomposition reaction. With the high oxidation potential of the hydroxyl radical that is produced in the Fenton reaction, various organic pollutants could be degraded [35,41]. Fig. 5 shows the conversion of phenol over the various as-prepared products under the visible light irradiation for 4 h or in the dark condition. From the data in Fig. 5, we can conclude that the order of decomposition rates for all samples are BCMS2 + H_2O_2 > BCMS2 > BCMS1 > BCMS2 + H_2O_2, dark > BCMS2, dark. It is obvious that the Fenton reagent, H_2O_2 and Fe^{2+} ions, increase the reactive rate of the decomposition of the phenol solution. This confirmed that both the photocatalyst and Fenton reagent contributed to the decomposition of the phenol. More importantly, the complex magnetic nanocomposite could be

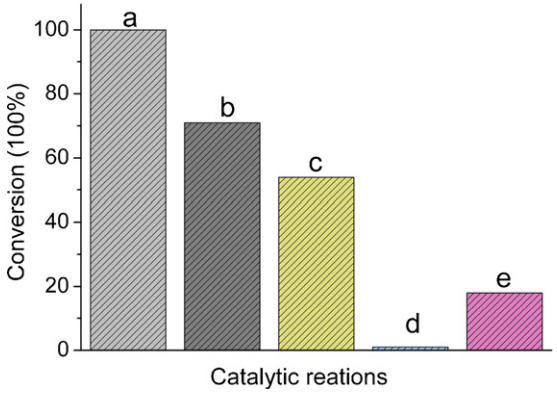

Fig. 5. Photocatalytic conversion of phenol over the as-prepared products with different conditions: (a) BCMS2 and H_2O_2 used as photocatalyst; (b) BCMS2 used as photocatalyst; (c) BCMS1 used as photocatalyst; (d) BCMS2 used as photocatalyst, without the light irradiation; (e) BCMS2 and H_2O_2 used as photocatalyst, without the light irradiation.

easily recovered from the solution by a magnet. This is advantageous considering its application in the water treatment.

4. Conclusion

In summary, Bi_2WO_6@carbon/Fe_3O_4 nanostructure with a thin carbon interlayer has been prepared by a three-step approach. The Bi_2WO_6 nanoplates could easily grow on the activated carbon layer coating on the Fe_3O_4 microsphere. The activated carbon layer was proved as an essential "bond" for combining two materials with different crystalline structure. Test results of the phenol decomposition indicate that the amount of the Bi_2WO_6 nanoplates affected its photocatalytic efficiency and the addition of H_2O_2 improved the efficiency of the phenol decomposition. Photocatalysis, magnetism and advanced oxidation were involved into a unit as a multifunctional nanocomposite. The proposed strategy for the preparation of complex nanostructures with multicomponent can be extended to other materials with similar structures.

Acknowledgements

We acknowledge the financial support from the National Natural Science Foundation of China (50672117, 50732004), National Basic Research Program of China (973 Program, 2007CB613305), and the Nanotechnology Programs of Science and Technology Commission of Shanghai Municipality (0852nm00500).

References

[1] J.H. Park, L. Gu, G. von Maltzahn, E. Ruoslahti, S.N. Bhatia, M.J. Sailor, Biodegradable luminescent porous silicon nanoparticles for in vivo applications, Nat. Mater. 8 (2009) 331–336.
[2] Q. Sun, Q. Wang, P. Jena, Y. Kawazoe, Design of janus nanoparticles with atomic precision: tungsten-doped gold nanostructures, ACS Nano 2 (2008) 341–347.
[3] V. Sharma, J. Jiang, M. Hossu, A.R. Koymen, S. Priya, Self-assembled periodic nanoporous network in multifunctional ZrO_2–CeO_2–$(La_{0.8}Sr_{0.2})MnO_3$ composites, Appl. Phys. Lett. 90 (2007), 123110-1-123110-3.
[4] C.L. Lo, K.M. Lin, C.K. Huang, G.H. Hsiue, Self-assembly of a micelle structure from graft and diblock copolymers: an example of overcoming the limitations of polyions in drug delivery, Adv. Func. Mater. 16 (2006) 2309–2316.
[5] M. Chen, Y.N. Kim, H.M. Lee, C. Li, S.O. Cho, Multifunctional magnetic silver nanoshells with sandwichlike nanostructures, J. Phys. Chem. C 112 (2008) 8870–8874.
[6] M. Chen, Y.N. Kim, C. Li, S.O. Cho, Preparation and characterization of magnetic nanoparticles and their silica egg-yolk-like nanostructures: a prospective multifunctional Nanostructure platform, J. Phys. Chem. C 112 (2008) 6710–6716.
[7] F. Caruso, M. Spasova, A. Susha, M. Giersig, Caruso, Magnetic nanocomposite particles and hollow spheres constructed by a sequential layering approach, Chem. Mater. 13 (2001) 109–116.
[8] E.M. Claesson, A.P. Philipse, Monodisperse magnetizable composite silica spheres with tunable dipolar interactions, Langmuir 21 (2005) 9412–9419.
[9] J.P. Fortin, C. Wilhelm, J. Servais, C. Menager, J.C. Bacri, F. Gazeau, Size-sorted anionic iron oxide nanomagnets as colloidal mediators for magnetic hyperthermia, J. Am. Chem. Soc. 129 (2007) 2628–2635.
[10] U. Jeong, X.W. Teng, Y. Wang, H. Yang, Y.N. Xia, Superparamagnetic colloids: controlled synthesis and niche applications, Adv. Mater. 19 (2007) 33–60.
[11] J. Kim, J.E. Lee, J. Lee, Y. Jang, S.W. Kim, K. An, J.H. Yu, T. Hyeon, Generalized fabrication of multifunctional nanoparticle assemblies on silica spheres, Angew. Chem. Int. Ed. 45 (2006) 4789–4793.
[12] H. Yu, M. Chen, P.M. Rice, S.X. Wang, R.L. White, S.H. Sun, Dumbbell-like bifunctional Au–Fe_3O_4 nanoparticles, Nano Lett. 5 (2005) 379–382.
[13] H.W. Gu, Z.M. Yang, J.H. Gao, C.K. Chang, B. Xu, Heterodimers of nanoparticles: formation at a liquid–liquid interface and particle-specific surface modification by functional molecules, J. Am. Chem. Soc. 127 (2005) 34–35.
[14] L. Zhang, Y.H. Dou, H.C. Gu, Synthesis of Ag–Fe_3O_4 heterodimeric nanoparticles, J. Colloid Interface Sci. 297 (2006) 660.
[15] K.W. Kwon, M. Shim, γ-Fe_2O_3/II–VI sulfide nanocrystal heterojunctions, J. Am. Chem. Soc. 127 (2005) 10269–10275.
[16] H.W. Gu, R. Zheng, X. Zhang, B. Xu, Facile one-pot synthesis of bifunctional heterodimers of nanoparticles: a conjugate of quantum dot and magnetic nanoparticles, J. Am. Chem. Soc. 126 (2004) 5664–5665.
[17] W.L. Shi, Y. Sahoo, H. Zeng, Y. Ding, M.T. Swihart, P.N. Prasad, Anisotropic growth of PbSe nanocrystals on Au–Fe_3O_4 hybrid nanoparticles, Adv. Mater. 18 (2006) 1889–1894.
[18] W.Y. Fu, H.B. Yang, M.H. Li, N. Yang, G.T. Zou, Anatase TiO2 nanolayer coating on cobalt ferrite nanoparticles for magnetic photocatalyst, Anatase TiO_2 nanolayer coating on cobalt ferrite nanoparticles for magnetic photocatalyst, Mater. Lett. 59 (2005) 3530–3534.
[19] S. Watson, D. Beydoun, R. Amal, Synthesis of a novel magnetic photocatalyst by direct deposition of nanosized TiO2 crystals onto a magnetic core, J. Photochem. Photobiol. A: Chem. 148 (2002) 303–313.
[20] S. Kurinobua, K. Tsurusakib, Y. Natuic, M. Kimatac, M. Hasegawa, Decomposition of pollutants in wastewater using magnetic photocatalyst particles, J. Magn. Magn. Mater. 310 (2007) e1025–1027.
[21] W.L. Kostedtiv, J. Drwiega, D.W. Mazyck, S.W. Lee, W. Sigmund, C.Y. Wu, P. Chadik, Magnetically agitated photocatalytic reactor for photocatalytic oxidation of aqueous phase organic pollutants, Environ. Sci. Technol. 39 (2005) 8052–8056.
[22] F. Caruso, Nanoengineering of particle surfaces, Adv. Mater. 13 (2001) 11–22.
[23] R.A. Caruso, M. Antonietti, Sol–gel nanocoating: an approach to the preparation of structured materials, Chem. Mater. 13 (2001) 3272–3282.
[24] J. Zhang, H.L. Zou, Q. Qing, Y.L. Yang, Q.W. Li, Z.F. Liu, X.Y. Guo, Z.L. Du, Effect of chemical oxidation on the structure of single-walled carbon nanotubes, J. Phys. Chem. B 107 (2003) 3712–3718.
[25] D.B. Mawhinney, V. Naumenko, A. Kuznetsova, J.T. Yates, J. Liu, R.E. Smalley, Infrared spectral evidence for the etching of carbon nanotubes: ozone oxidation at 298 K, J. Am. Chem. Soc. 122 (2000) 2383–2384.
[26] H.C. Choi, M. Shim, S. Bangsaruntip, H.J. Dai, Spontaneous reduction of metal ions on the sidewalls of carbon nanotubes, J. Am. Chem. Soc. 124 (2002) 9058–9059.
[27] B.S. Kong, D.H. Jung, S.K. Oh, C.S. Han, H.T. Jung, Single-walled carbon nanotube gold nanohybrids: application in highly effective transparent and conductive films, J. Phys. Chem. C 111 (2007) 8377–8382.
[28] L.T. Qu, L.M. Dai, Substrate-enhanced electroless deposition of metal nanoparticles on carbon nanotubes, J. Am. Chem. Soc. 127 (2005) 10806–10807.
[29] A. Kudo, S. Hijii, H_2 or O_2 evolution from aqueous solutions on layered oxide photocatalysts consisting of Bi^{3+} with $6s^2$ configuration and d^0 transition metal ions, Chem. Lett. 10 (1999) 1103–1104.
[30] J.W. Tang, Z.G. Zou, J.H. Ye, photocatalytic decomposition of organic contaminants by Bi_2WO_6 under visible light irradiation, Catal. Lett. 92 (2004) 53–56.
[31] K.R. Kendall, C. Navas, J.K. Thomas, H.C. Loye, Recent developments in oxide ion conductors: aurivillius phases, Chem. Mater. 8 (1996) 642–649.
[32] Y. Tsunoda, M. Shirata, W. Sugimoto, Z. Liu, O. Terasaki, K. Kuroda, Y. Sugahara, Preparation and HREM characterization of a protonated form of a layered perovskite tantalate from an aurivillius phase $Bi_2SrTa_2O_9$ via acid treatment, Inorg. Chem. 40 (2001) 5768–5771.
[33] J.Y. Kim, I. Chung, J.H. Choy, G.S. Park, Macromolecular nanoplatelet of aurivillius-type layered perovskite oxide: $Bi_4Ti_3O_{12}$, Chem. Mater. 13 (2001) 2759–2761.
[34] Y. Tsunoda, W. Sugimoto, Y. Sugahara, Intercalation behavior of *n*-alkylamines into a protonated form of a layered perovskite derived from aurivillius phase $Bi_2SrTa_2O_9$, Chem. Mater. 15 (2003) 632–635.
[35] A. Vogelpohl, S.M. Kim, Advanced oxidation processes (AOPs) in wastewater treatment, J. Ind. Eng. Chem. 10 (2004) 33–40.
[36] H. Lim, J.W. Lee, S. Jin, J.Y. Kim, J.Y. Yoon, T. Hyeon, Highly active heterogeneous Fenton catalyst using iron oxide nanoparticles immobilized in alumina coated mesoporous silica, Chem. Commun. 4 (2006) 463–465.
[37] H. Deng, X.L. Li, Q. Peng, X. Wang, J.P. Chen, Y.D. Li, Monodisperse magnetic single-crystal ferrite microspheres, Angew. Chem. Int. Ed. 44 (2005) 2782–2785.
[38] X.M. Sun, Y.D. Li, Colloidal carbon spheres and their core/shell structures with noble-metal nanoparticles, Angew. Chem. Int. Ed. 43 (2004) 597–601.
[39] L.B. Luo, S.H. Yu, H.S. Qian, J.Y. Gong, Large scale synthesis of uniform silver@carbon rich composite (carbon and cross-linked PVA) sub-microcables by a facile green chemistry carbonization approach, Chem. Commun. 7 (2006) 793–795.
[40] Z. He, C. Sun, S.G. Yang, Y.C. Ding, H. He, Z.L. Wang, Photocatalytic degradation of rhodamine B by $Bi_2WO_6$with electron accepting agent under microwave irradiation: Mechanism and pathway, J. Hazard. Mater. 162 (2009) 1477–1486.
[41] Y.L. Nie, C. Hu, Jiuhui Qu, X.X. Hu, Efficient photodegradation of Acid Red B by immobilized ferrocene in the presence of UVA and H_2O_2, J. Hazard. Mater. 154 (2009) 146–152.